DEVELOPMENT OF HIGH-THROUGHPUT SCREENING METHOD FOR IRON TRANSPORT INHIBITORS IN E. COLI

by

MATHEW HANSON

B.S., Southwestern College, 2009

A THESIS

submitted in partial fulfillment of the requirements for the degree

MASTER OF SCIENCE

Department of Biochemistry and Molecular Biophysics
College of Arts and Sciences

KANSAS STATE UNIVERSITY
Manhattan, Kansas

2015

Approved by:

Major Professor
Dr. Phillip Klebba

Copyright

Abstract

Iron acquisition is a component of Gram-negative bacteria pathogenesis, therefore as a form of 'nutritional immunity' host organisms sequester iron. To obtain iron bacteria secrete siderophores that scavenge *iron. Th*e E. coli outer membrane protein FepA actively transports the siderophore ferric enterobactin into the periplasm. We observe this uptake reaction by fluorescently labeling FepA in live bacteria, monitoring quenching that occurs upon binding of FeEnt, and then fluorescence recovery during transport. Energy poisons azide, arsenate, and 2,4-dinitrophenol were evaluated to determine sensitivity to known transport inhibitors. We developed and optimized methods to screen for iron transport inhibitors using a cell-based high-throughput screening platform. These inhibitors may have broad spectrum bacteriostatic antibiotic properties.

Table of Contents

List of Figures

List of Tables

Acknowledgements

I would like to thanks all those who have made this possible including Dr. Phillip Klebba, Dr. Sally Newton, my lab colleagues, and supervisory committee. Also, without the support of my family and Kristin I would not have been able to finish this project.

Chapter 1 - Introduction

Gram-Negative Bacteria

130 years ago Christian Gram developed what is now known as Gram staining to broadly classify bacteria into two groups. Gram-positive bacteria retain the crystal violet stain while Gram-negative do not. The structural differences in the cell envelope is the basis for this property. Both groups contain a cellular membrane and a peptidoglycan layer, however Gram-negative bacteria also contain a second membrane forming the outermost layer (Figure 1-1).[1] Peptidoglycan is a polymer of disaccharides and amino acids forming a rigid and generally impermeable protective mesh.[2] Although both classifications contain a peptidoglycan layer, gram-negative bacteria have a thinner layer than gram-positive bacteria.[1] The space between the inner and outer membranes that contains the peptidoglycan layer is known as the periplasm. This periplasmic space also contains a large number of proteins that facilitate many important functions for the cell.[1]

The protective outer membrane contributes to Gram-negative bacteria generally being more resistant to antibiotics than Gram-positive bacteria. *Escherichia coli, Neisseria meningitidis, Pseudomonas aeruginosa, and Helicobacter pylori* are all medically relevant bacteria with gram-negative morphology.[3]

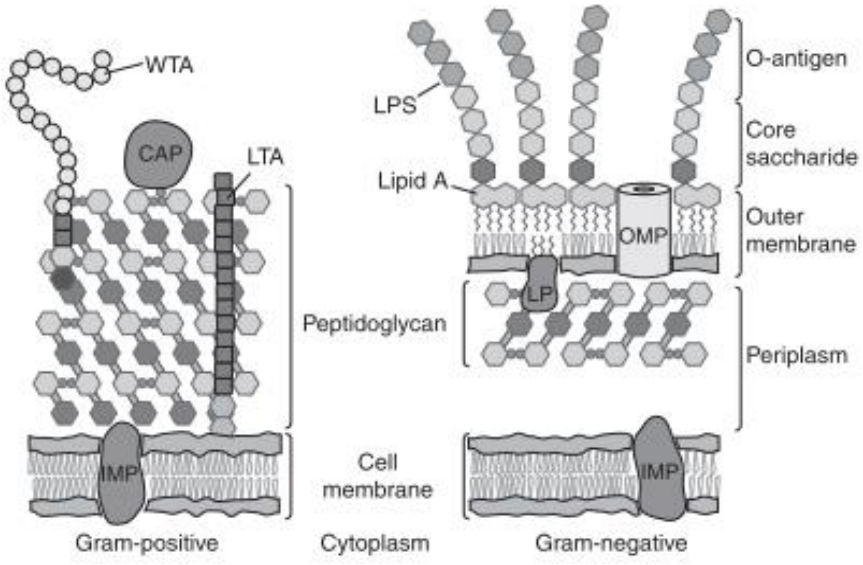

Figure 1-1 Gram-positive and Gram-negative cell envelopes

WTA = wall teichoic acid; CAP = covalently attached protein; LTA = lipoteichoic acid; LPS = lipopolysaccharide; OMP = outer membrane protein; LP = lipoprotein; IMP = integral membrane protein.[1]

The bacterial cell envelope provides protection from the extracellular environment, allows nutrients into the cell, and waste out of the cell.[1] The membrane performs many other essential cellular processes such as energy production and lipid biosynthesis.[1]

Iron

Iron represents a vital nutrient for bacteria due to its role in many cellular processes such as energy production, DNA synthesis, and nitrogen fixation.[4] The

ability of iron to serve as a catalyst comes from the two forms of the element, ferrous (Fe^{2+}) and ferric (Fe^{3+}) iron; this allows iron be used in many reactions as a co-factor of many proteins.[5] Nitrogenase, hydrogenase, peroxidase, superoxide dismutase, glutamate synthase, and cytochrome all require iron to function.[4] Within these proteins, iron can exist in different forms as a co-factor (heme, iron-sulfur clusters, and free iron).

Iron is also highly regulated due to the toxicity of the reduced form.[4] As a result in biological systems iron is often complexed by other molecules as a co-factor or in storage.[5] Eukaryotic organisms store iron in many forms such as ferritin.[6]

Despite being one of the most abundant elements, iron is scarce at physiological conditions due to rapid oxidation to an insoluble form.[7] The concentration of available iron can be as low as 10^{-9} M in an aqueous environment.[8] To overcome this scarcity bacteria utilize several strategies to obtain iron. Hemophore proteins scavenge for heme and bind heme complexes.[8] Bacteria also secrete low molecular weight compounds known as siderophores that bind ferric iron.[9] Enterobactin, a 700 dalton siderophore for many Gram-negative bacteria has the strongest known affinity for iron ($K = 10^{52}$ M^{-1}) (Figure 1-2).[7]

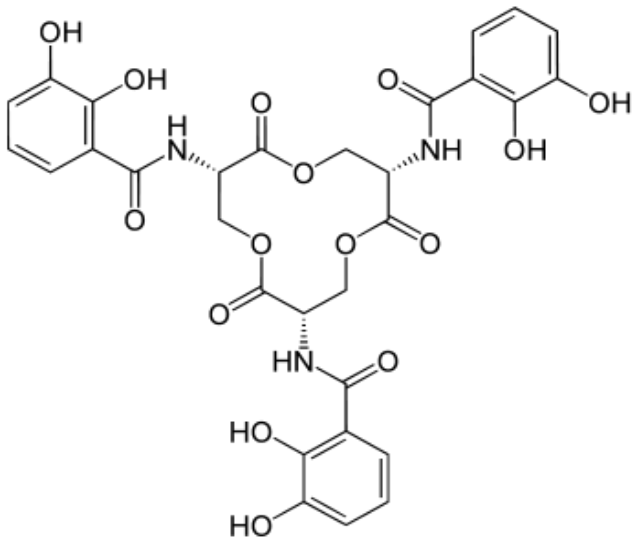

Figure 1-2 Enterobactin structure

Native siderophore of *E. coli* binds ferric iron.[10]

FepA

After iron is bound to the siderophore, ferric enterobactin (FeEnt), the bacterium still must internalize the complex to fulfill their nutritional requirements. The first step involves crossing the outer membrane of the gram-negative bacteria. Due to the size of ferric enterobactin (719 Da), the molecule can't pass through the outer membrane porins and requires a specific transporter.[5,11] The outer membrane transporter protein for enterobactin in *E. coli* is FepA (Figure 1-3).[12] This 724 residue ligand-gated porin contains a 22 strand antiparrallel β-barrel that spans the outer membrane with an N-terminal plug domain that occludes the barrel.[12]

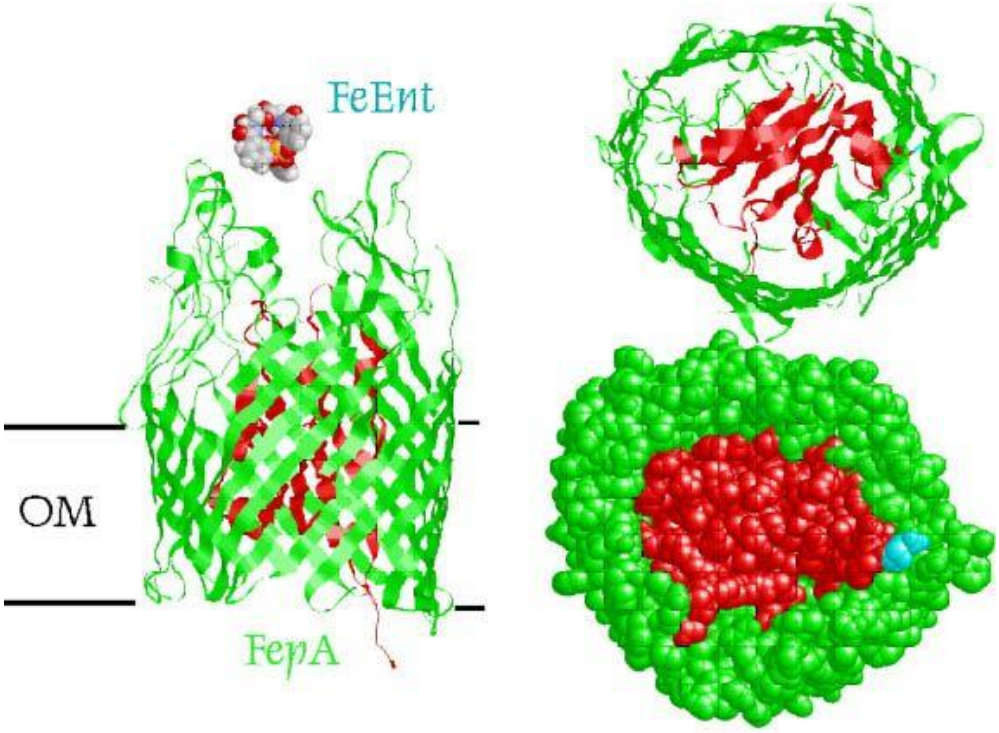

Figure 1-3 FepA Structure

Crystal structure of FepA with FeEnt shown from side and periplasm views. N-terminal globular domain is depicted in red. TonB binding domain is depicted in cyan.[12]

Transport of FeEnt through FepA has not been completely resolved, but the 11 flexible loops on the extracellular side of FepA play a role in the reaction.[13,14] The second step in the biphasic transport process is the rate-limiting step.[15] Upon FeEnt binding the extracellular loops of FepA shift from an open to a closed conformation around FeEnt that allows for transport.[14] The paradox of FeEnt transport involves the passage of FeEnt through a blocked β-barrel. The N-terminal domain must be displaced in some way for FeEnt passage into the periplasm. Several models for the

movement of the N-terminal domain have been theorized.[16] Ejection of the N-terminal domain into the periplasm while folded, partially folded, or unfolded would allow for transport across the β-barrel.[16] Another model suggests the N-terminal domain changes conformation but does not move into the periplasm.[16] The proposed temporary channel enables transport of FeEnt across FepA.[16]

TonB-Dependent Transport

Transport across the outer membrane via FepA is an energy dependent process, and as such the membrane architecture of Gram-negative bacteria poses a challenge.[17] How can the cell power active transport processes in the outer membrane when porins, such as OmpF, prevent establishing an energy gradient across the outer membrane due to diffusion of the high-energy compounds.[11]

Gram-negative bacteria have evolved an active transport system that couples transport across the outer membrane to energy transduction across the inner membrane (Figure 1-4).[18] The protein complex of TonB-ExbB-ExbD along with TonB-dependent outer membrane proteins, such as FepA, form this system.[18] TonB spans the periplasm and interacts with TonB-dependent proteins at a conserved site known as the 'TonB box'.[12] In FepA this site consists of amino acid residues 12-18.[12] ExbB and ExbD stabilize TonB and provide the energy for interaction by utilizing the proton motive force across the inner membrane.[19]

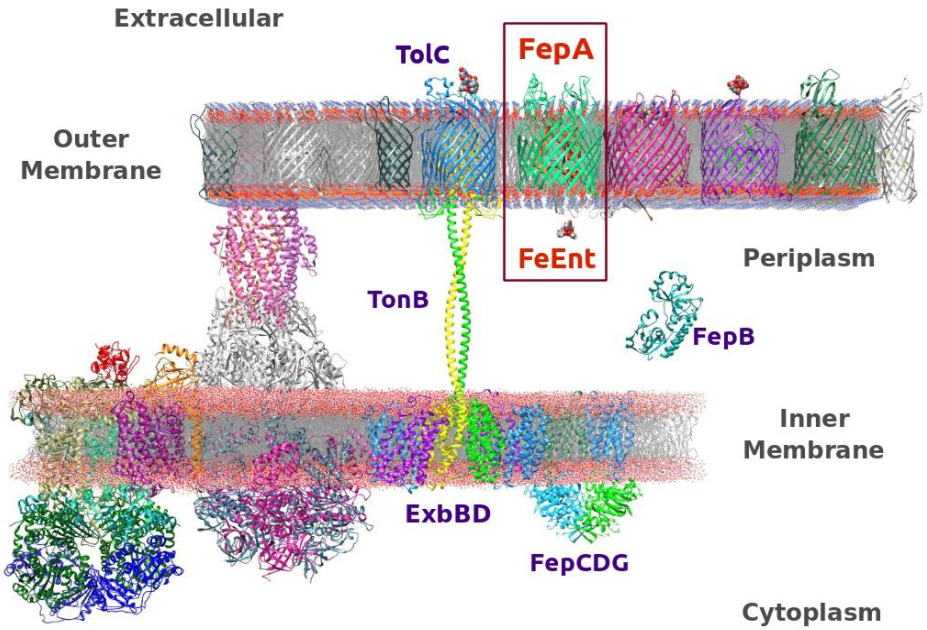

Figure 1-4 Depiction of Gram-negative bacterial cell envelope architecture

Representation of membrane architecture with iron acquisition proteins and other membrane proteins (figure from PE Klebba).

The interaction between TonB-dependent transporters and TonB is not fully elucidated. However, the FeEnt binding to FepA induces a conformational shift in FepA that is transmitted to the periplasm via the TonB Box.[20,21] After TonB interacts with FepA to allow passage into the periplasm FeEnt binds to FepB.[22] This periplasmic protein transports FeEnt to the inner membrane protein complex of FepC-FepD-FepG.[23,24] FepC hydrolyzes cytoplasmic ATP to enable transport across the inner membrane, and FepD/FepG form the pore within the inner membrane.[23,24]

High-Throughput Screening

In less than 30 years high-throughput screening (HTS) has emerged as a vital tool for the pharmaceutical industry and many other fields. Prior to the development of HTS, drug discovery methods were limited to testing fewer than 50 compounds per week; now the screening capabilities of ultra-high throughput instrumentation exceeds 100,000 compounds screened per day.[25] Advances in combinatorial chemistry have enabled the creation of chemical libraries required for such large screening campaigns.[25] Robotic automation and acoustic liquid dispensing have also contributed to the rapid increase in screening throughput. Newer plate designs decrease reagent costs and allow for faster sampling by decreasing well size. 384, 1536, and 3456 well formats have largely replaced the standard 96 well plate. The use of HTS has also expanded from primarily the pharmaceutical industry to academic settings. Modern HTS instruments are capable of utilizing bioluminescence, fluorescence, reporter genes, calcium mobilization, and label-free detection methods.

One type of HTS screening, biochemical assays, often involves a purified protein and ligand binding assay. This format allows for an increased signal compared to cell-based assays; however, cell-based assays generate more physiologically relevant data.[26] This is increasingly important in the pharmaceutical industry due to the cost of late stage clinical failures.[27] An increased focus on ADMET (absorption, distribution, metabolism, excretion and toxicity) in screening has been adopted to help prevent these failures.[28] The power of HTS is illustrated by the discovery of the drug Torcetrapib as the screening campaign found only one hit after testing over 350,000 compounds.[25]

Previous Studies

Numerous studies have been performed on FepA, enterobactin, and Gram-negative bacterial iron acquisition system. The basis for many of these studies is site-directed mutagenesis of FepA. This technique allows for cysteine substitution mutations in various locations within the protein.[16] Labeling the mutant residues with fluorescent probes allows for high sensitivity monitoring during FeEnt transport.[17] Specific labeling of these residues is possible as FepA only has 2 native cysteine residues that exist in a disulfide bond, and cysteine residues are relatively rare among outer membrane proteins.[12] After optimizing the labeling conditions over 75 cysteine mutants have been created, and the effects of fluorescent labeling on binding and transport has been evaluated (Figure 1-5).[16]

The changes in the excitation/emission spectra during FeEnt transport help explain the conformational shifts of FepA. The 7 extracellular loops of FepA move from an open to closed conformation around FeEnt upon binding.[14] This is observed by the quenching of fluorescence as the local environmental changes around fluorophore are conferred to shifts in the spectral properties.[29] It has been shown that the extracellular loops close around the FeEnt in a sequential manner.[29]

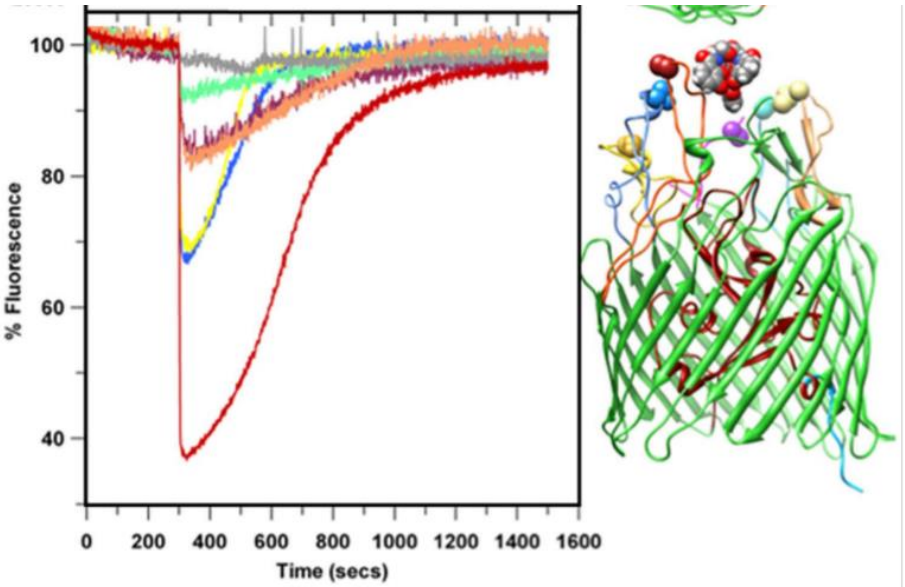

Figure 1-5 FepA cysteine mutants fluorescence profiles

Fluorescence quenching and recovery of fluorescence maleimide labeled extracellular loops of FepA after FeEnt addition at 300 seconds.[29]

The susceptibility of the mutants to labeling is dependent on their accessibility to the extracellular environment or the periplasm at the time of labeling.[29] Dual mutants can form disulfide bridges under oxidizing conditions and the impact on protein function/conformation can be assessed.[16]

Importance

Antibiotic resistance represents one of the greatest challenges in modern medicine.[30] Once treatable diseases now require escalating classes of antibiotics, and even drugs of last resort have resistant strains.[30] Besides the increased mortality due to

ineffective treatment, the cost of resistance reaches billions of dollars in increased medical costs.[30] Resistance arises quickly as it is highly motile between bacteria and with or without antibiotic selection pressure the loss of resistance is slow.[30] The misuse of antibiotics is one reason for the increase in antibiotic resistance.[3] This is one consequence of the increased usage of antibiotics in the medical and agricultural industries.

One strategy to fight antibiotic resistance is to create new antibiotics. Structurally similar drugs or drugs that target the same mechanisms are more likely to become ineffective, making drugs that affect new targets especially promising.[3] Due to iron's importance to bacterial growth and pathogenicity, an inhibitor of TonB-dependent iron acquisition could have novel antibiotic properties.[8]

Finding inhibitors of TonB may also have theoretical importance as the FeEnt/FepA transporter is typical of many other Gram-negative outer membrane metal transporters.[31] Finding additional ligands for FepA may also help elucidate the transport mechanisms of the protein which has yet to be completely resolved.

Research Conducted in this Study

The aim of this study was to convert and optimize previously developed low-throughput methods of measuring iron transport for a high-throughput platform and ultimately to find inhibitors of TonB-dependent iron transport. Using fluorescently labeled cells, transport of ferric enterobactin through FepA was observed via fluorescence quenching and recovery.

In the first part of this study three different energy poisons (azide, arsenate, and 2,4-dinitrophenol (DNP)) were tested to determine their IC_{50} values. Given that FeEnt is an energy dependent process, this pathway is sensitive to disruption of the bacterial cellular energy supply, and as a result iron transport is inhibited. In the absence of any known inhibitor of FepA, the energy poisons serve as a control in the second part of the study. Low throughput data also served as a proof-of-concept prior to HTS testing.

The second part of the study involves the development of the HTS method. Several parameters (cell concentration, FeEnt concentration, control stability, and cell stability) were optimized. This novel assay measures the fluorescence of bacterial cells before and after addition of FeEnt, and ultimately monitors transport of the ferric siderophore. Using this microtiter assay we observe TonB-dependent transport and we can identify inhibitor of that process. Z-factor calculations to determine the viability of the method were performed, and show the assay can produce statistical significance data.

Chapter 2 - Materials

Strains

E. coli strain OKN3 (*ΔfepA*) with plasmid pITS23 were used for all tests. This low-copy plasmid contained FepA cysteine substitution mutant S271C. Mutant *fepA* were under the native repressible fur promoter.

Instrumentation

Energy poison and low-throughputs studies were performed using SLM 8000 spectrofluorometer upgraded to SLM 8100 (Aminco, USA). 440 nm and 480 nm were used as the excitation and emission wavelengths. High-throughput screening development assays were performed on Tecan GENios Pro with black round-bottom 96 well plates (Tecan, Switzerland) (Corning, USA). 485 nm and 535 nm were used as the excitation and emission wavelengths.

Chapter 3 - Methods

Fluorescent Labeling

We adapted previously described methods to fluorescently label cysteine residues in FepA.[17] After inoculating cells into LB for 12 hours, we subcultured the cells into MOPS media for 5.5 to 6 hours, until mid-log phase (4-5 x 10^8 cells mL^{-1}). Streptomycin (50 µg/mL) and chloremphenicol (20 µg/mL) were used as antibiotics in LB and MOPS media. We collected the cells via centrifugation and resuspended in 50 mM $NaHPO_4$, pH 6.5 twice. Fluorescein maleimide was added to the cells for 5 minutes at 5 µM. Labeling was quenched by adding 1.3 mM 2-mercaptoethanol. We collected cells via centrifugation and resuspended in phosphate buffered saline (PBS) twice. Cell concentration was determined using optical density at 600 nm.

Energy Poisons

The previously described labeled cells were incubated at 37°C for 30 minutes with an energy poison (azide, arsenate, or DNP) at the appropriate concentration. We added 5% ethanol to DNP samples for solubility. Cells were diluted to a concentration of 2.5 x 10^7 cells mL^{-1} with PBS and 4% glucose and then analyzed with moderate mixing. We performed energy poison studies using a 2 mL sample volume in a SLM 8000 fluorospectrophotometer upgraded to SLM 8100 (Aminco, USA). After fluorescence readings stabilized FeEnt was added at the indicated concentrations, and transport of FeEnt was monitored. We performed all samples in triplicate and the data

was normalized to account for variation inherent to the assay. Data analysis was performed using GraFit 6.0 (Erithacus Software Ltd.).

FeEnt Dilutions

Labeled cells were incubated at 37°C for 30 minutes. We diluted cells to a concentration of 2.5 x 10^7 cells mL^{-1} with PBS and 4% glucose and then analyzed with moderate mixing. Measurements were performed using a 2 mL sample volume in a SLM 8000 fluorospectrophotometer upgraded to SLM 8100 (Aminco, USA). We added FeEnt at the indicated concentration (1 to 32 nM) after fluorescence readings stabilized, and transport of FeEnt was then monitored. All samples were performed in triplicate and the data was normalized to account for variation inherent to the assay. We performed data analysis using GraFit 6.0.

Cell Dilution

The rate of depletion of extracellular FeEnt was measured over a wide range dilution of cell densities using Tecan GENois Pro. We added labeled cells in triplicate to a 96 well plate at decreasing densities (0.250 to 0.007 cells/mL ($x10^8$)) with a total well volume of 190 µL. Cells were diluted with PBS and we added 4% glucose solution as an energy source. Fluorescence gain was determined prior measurements with 485 nm and 535 nm the excitation and emission wavelengths. After measuring unquenched fluorescence, FeEnt was added to all wells using the Tecan automatic injectors. We used a FeEnt concentration of 200 nM to ensure maximal fluorescence quenching

across all cell densities. The plate was then shaken for 10 seconds prior to measuring the FeEnt transport time course over 110 minutes. We performed data analysis using GraFit 6.0.

Cell Density

The effect of cellular density on assay Z-factor was measured using Tecan GENois Pro. We added labeled cells in triplicate to a 96 well plate at varying densities (0.01 to 0.5 cells/mL ($x10^8$)) with a total well volume of 190 µL. Cells were diluted with PBS, and we added 4% glucose solution as an energy source. We analyzed each cell concentration separately to maximize instrument sensitivity. Fluorescence gain was determined prior to adding FeEnt with 485 nm and 535 nm as the excitation and emission wavelengths. After measuring unquenched fluorescence for 5 cycles, 10 µL FeEnt was added to all wells using the Tecan automatic injectors. Concentration of FeEnt corresponds to cell density to ensure the same FeEnt/cells ratio. The plate was then shaken for 10 seconds prior to measuring the FeEnt transport time course over 20 minutes. We performed data analysis using GraFit 6.0.

FeEnt Dilutions

FeEnt concentration ranging from 2 nM to 40 nM were evaluated using Tecan GENois Pro. We added labeled cells (0.1 cells/mL ($x10^8$)) to black 96 well plates in triplicate. Fluorescence gain was determined prior adding FeEnt with 485 nm and 535 nm as the excitation and emission wavelengths. After measuring unquenched

fluorescence for 5 cycles, FeEnt at indicated concentration was added to all wells using the Tecan automatic injectors. The plate was then shaken for 10 seconds prior to measuring the FeEnt transport time course over 50 minutes. We performed data analysis using GraFit 6.0.

Z-Factor

We used Z-factor calculations to determine the statistical significance of the HTS results and the viability of assay.[32] To determine the statistical effect size the positive and negative controls were used in the calculations.

$$\text{Z-factor} = 1 - \frac{3(\sigma_p + \sigma_n)}{|\mu_p - \mu_n|}$$

Cell Stability

The ability of cells to transport FeEnt was measured over 9 hours using Tecan GENois Pro. We labeled cells as previous described and stored on ice. Aliquots samples of 0.1 cells/mL ($x10^8$) were tested in triplicate at 5 time points (0, 1, 3, 5, and 9 hours). After measuring unquenched fluorescence, 20 nM FeEnt was added to all wells using the Tecan automatic injectors. The plate was then shaken for 10 seconds prior to measuring the FeEnt transport time course over 95 cycles. We performed data analysis using GraFit 6.0.

Control Stability

The stability of the assay controls was measured over 1 hour using Tecan GENois Pro. Positive control 1 injected PBS without FeEnt after 5 cycles. In positive control 2, cells were incubated with 0.02 mM carbonyl cyanide *m*-chlorophenyl hydrazone (CCCP) for 30 minutes at 37°C. Negative control consisted of cells at 0.01 cells/mL ($x10^8$) without any energy poisons. Labeled cells (0.1 cells/mL ($x10^8$)) were added to a 96 well plate with a total well volume of 190 µL. Cells were diluted with PBS and we added 4% glucose solution as an energy source. After measuring unquenched fluorescence for 5 cycles, FeEnt or PBS was added to all wells using the Tecan automatic injectors. The plate was then shaken for 10 seconds prior to measuring the FeEnt transport time course over 50 minutes. We performed data analysis using GraFit 6.0.

Chapter 4 - Results

SLM Results

The results from energy poison studies reveal that cell were most sensitive to energy depletion via DNP, with arsenate the least potent. All control samples without energy poisons present were shown to quench fluorescence upon adding FeEnt and recover fluorescence within 400 seconds. For azide 18 mM was required to fully inhibit transport, and the IC_{50} value was 9 mM (Figure 4.1). For arsenate 180 mM was required to fully inhibit transport, and the IC_{50} value was 90 mM (Figure 4.2). Ethanol was added to control and experimental samples at 5% for solubility of DNP. For DNP 1.5 mM was required to fully inhibit transport, and the IC_{50} value was 0.75 mM (Figure 4.3). Two other energy poisons, CCCP and cyanide, were tested previously.[29] The results of all five energy poisons are summarized in Table 4.1 and all concentrations tested in this study in Table A.1.

To determine the effect of increasing concentrations of FeEnt on the fluorescence properties of iron transport via FepA we tested FeEnt at several concentrations (1, 2, 4, 8, 16, and 32 nM) (Figure 4.4). The extent of fluorescence quenching was found to be directly related to the amount of FeEnt added, up to 16 nM. With both 16 nM and 32 nM the maximal extent of fluorescence quenching was observed. The rate of depletion of extracellular FeEnt was observed by the recovery of fluorescence after quenching. This was found to be inversely related the amount of FeEnt added. Concentrations below 8 nM all fully transported FeEnt within 500 seconds. 16 nM samples exhibited minimum fluorescence recovery over 500 seconds, and 32 nM samples showed no recovery over 500 seconds.

Using the low-throughput fluorescence platform of the SLM we developed a framework for a high-throughput screening assay for inhibitors of TonB-dependent iron transport. By measuring fluorescence 3 times, instead of several times a second as in the SLM, transport can be evaluated in a high-throughput format. The three measurement times, as shown in Figure 4.5 with black rectangles, occur before addition of FeEnt, after addition of FeEnt, and after allowing for transport of FeEnt. Three possible controls were used to illustrate the assay concept. Addition of PBS without FeEnt at time 0, illustrate when FepA binding is prevented. Addition of 180 mM arsenate with cells illustrates when binding occurs but transport of FeEnt is prevented. Cells without energy poisons added represent normal binding and transport. By evaluating the statistical significant differences these three points the three outcomes after FeEnt addition can be differentiated in a high-throughput platform.

Tecan Results

Compared to the low-throughput platform of the SLM instrumentation the high-throughput Tecan instrumentation allows for more testing methodologies. Instead of a single cuvette, 96 or 384 samples can be tested simultaneously. We evaluated the relationship between cell density and FeEnt concentration using a serial cell dilution from 0.250 to 0.007 cells/mL ($x10^8$) (Figure 4.6). With a constant FeEnt concentration for all samples of 200 nM the ratio of extracellular FeEnt to FepA was dependent on the cell density. All samples had quenched fluorescence in the readings after FeEnt injection. The cell density was directly related to the rate of fluorescence recovery in the samples. At 0.250 cells/mL ($x10^8$) fluorescence recovered after 40 minutes but in more

dilute samples such as 0.007 cells/mL ($x10^8$) minimal fluorescence recovery was observed. The relationship between cell concentration and signal intensity was also illustrated as the signal decreased as the number of cells in the well decreased.

To determine the optimal cell concentration for the high-throughput screening we evaluated samples over a wide range of cell densities (Figure 4.7). Z-factor calculations were performed using a data points before and after the injection of FeEnt. The FeEnt/cell ratio was kept constant to ensure for consistent quenching of fluorescence. Table 4.2 summarizes the concentrations tested. All samples concentrations greater than 0.01 cells/mL ($x10^8$) were found to have a Z-factor greater than 0.5. The most dilute sample with 0.01 cells/mL ($x10^8$) exhibited a Z-factor of only 0.38.

To determine the optimal concentration of FeEnt to be added to cells we tested concentration from 2 to 40 nM (Figure 4.8). The extent of quenching was found to be directly related to the amount of FeEnt added. 2 nM samples fluorescence quenched to approximately 85% of the original intensity. 40 nM samples fluorescence quenched to approximately 40% of the original intensity. The consistency of the quenching and fluorescence equilibrium regions was also observed with minimal variation. In between these regions, the fluorescence recovery was found to be more variable, especially at higher concentrations of FeEnt as shown by error bars. The results also confirm those found using the SLM that increasing the concentration of FeEnt decreased the rate of fluorescence recovery. 2 nM samples recovered almost immediately, but 40 nM samples had not fully recovery after 3000 seconds.

High-throughput screening often lasts several hours so we sought test the stability of labeled cells over such a time frame. We stored cells on ice and aliquots were taken at the indicated time points over 9 hours and analyzed on the Tecan (Figure 4.9). Our results show that the samples were still able to transport FeEnt 9 hours after labeling while stored on ice. All samples exhibited quenched fluorescence approximately 40% of the original intensity. Very little variation was found in the speed of fluorescence recovery with all samples recovering fluorescence intensity within 400 seconds.

To determine the statistical viability and control stability of the assay in the Tecan, Z-factor calculations were performed on the three control samples over 3000 seconds (Figure 4.10). 0 nM FeEnt samples exhibited stable fluorescence over the entire timescale with little variation. Samples with CCCP (0.02 mM) and without CCCP both had quenched fluorescence after the addition of 20 nM FeEnt. CCCP samples had no recovery of fluorescence over 50 minutes. Samples without energy poisons recovered fluorescence and maintained that fluorescence intensity for approximately 25 minutes. Z-factor calculations were performed between all three controls at every data point. No statistical difference exists between the three controls before the injection, but after injection samples with FeEnt exhibit a Z-factor of at least 0.5 when compared to the 0 nM FeEnt control. Prior to recovery of fluorescence in the 0 mM CCCP sample no statistical difference exists when compared to the 0.02 mM CCCP sample. After recovery at approximately 1500 seconds, all samples are statistically different from one another and maintain this for 1500 seconds. These high Z-factors indicate that

significance statistical differences exist between all control samples when measured at three time points.

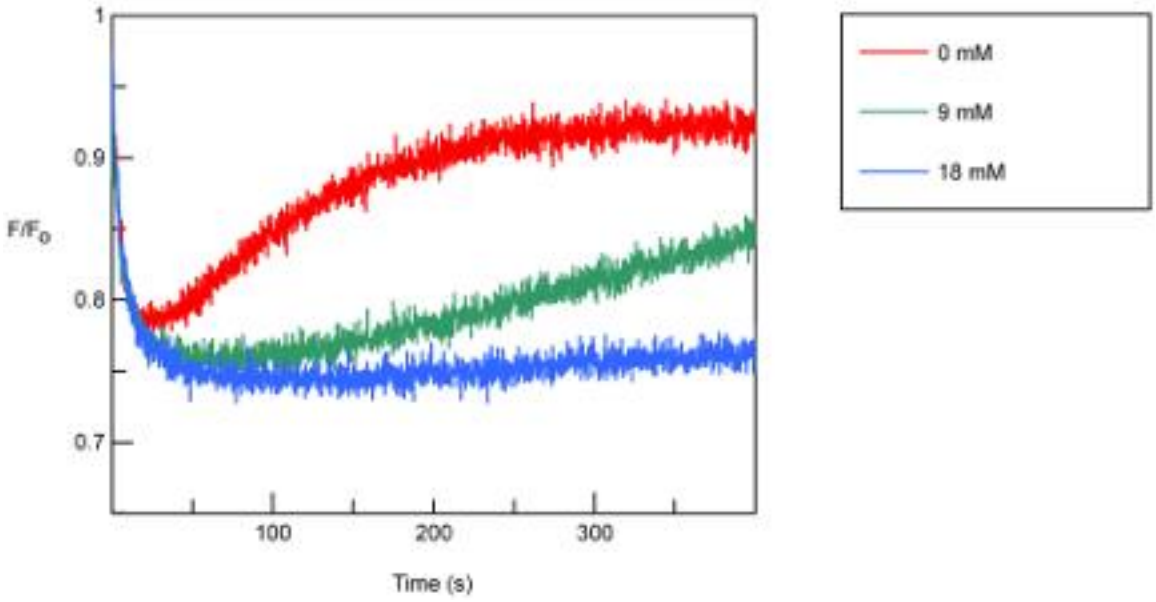

Figure 4.1 Inhibition of FeEnt transport by azide

We incubated OKN3/pFepAS271C cells with concentrations of sodium azide required for 50% inhibition (green) and 100% inhibition (blue) of fluorescence recovery caused via ferric enterobactin transport.

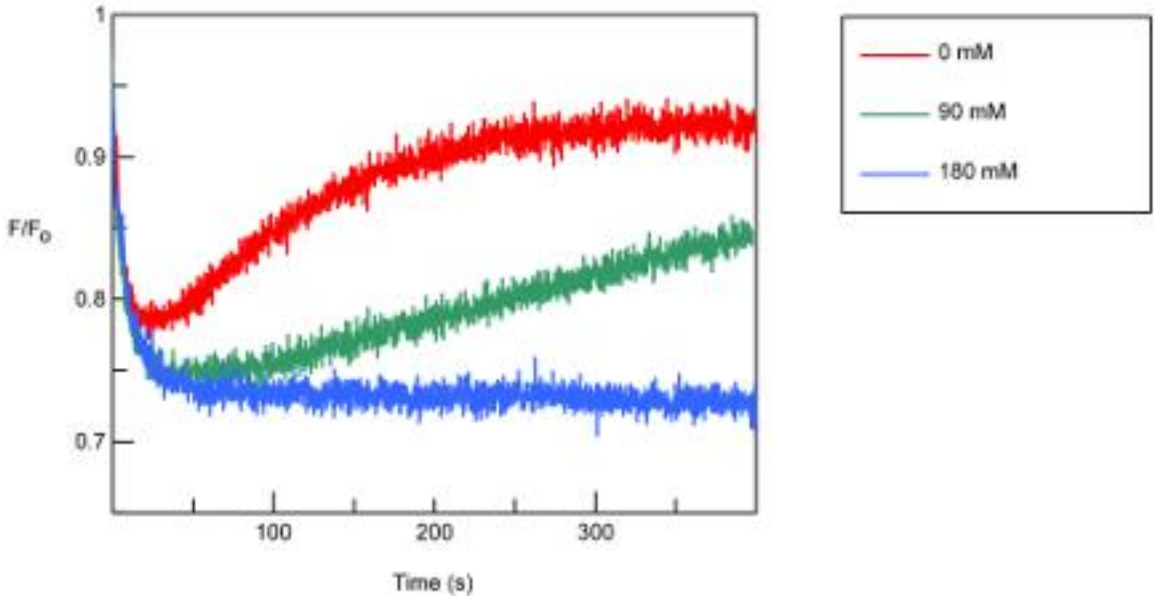

Figure 4.2 Inhibition of FeEnt transport by arsenate

We incubated OKN3/pFepAS271C cells with concentrations of arsenate required for 50% inhibition (green) and 100% inhibition (blue) of fluorescence recovery caused via ferric enterobactin transport.

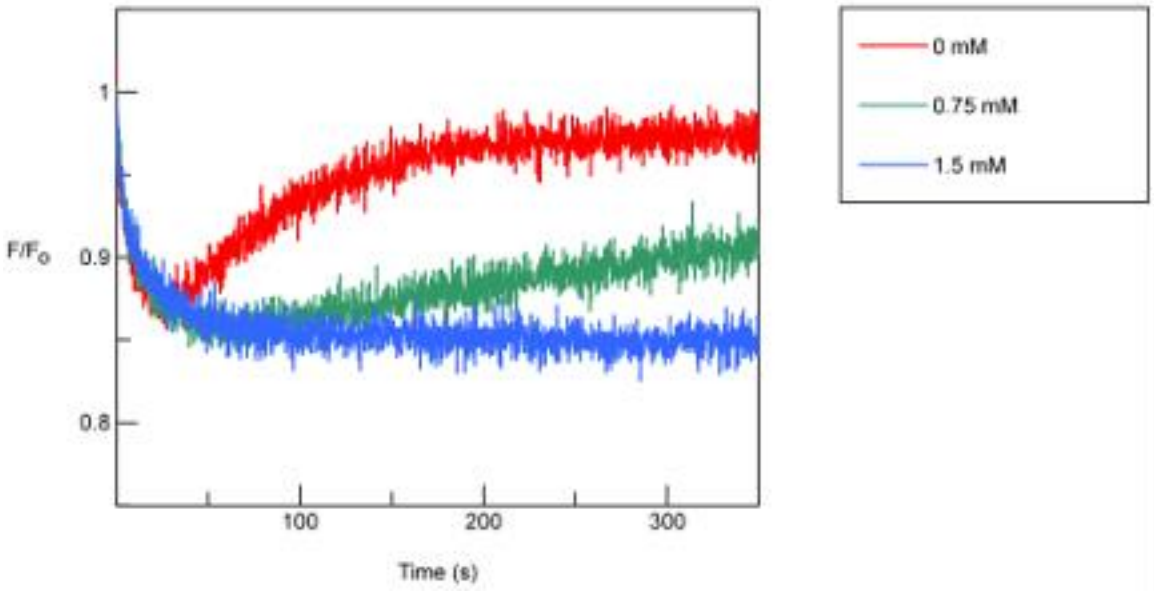

Figure 4.3 Inhibition of FeEnt transport by DNP

We incubated OKN3/pFepAS271C cells with concentrations of DNP required for 50% inhibition (green) and 100% inhibition (blue) of fluorescence recovery caused via ferric enterobactin transport.

Compound	Concentration (mM)	
	50% Inhibition	100% Inhibition
CCCP*	0.005	0.01
Cyanide*	2-3	5-6
Azide	9	18
Arsenate	90	180
DNP	0.75	1.5

Table 4-1 Energy poison summary

Summary of 50% and 100% inhibition concentrations of energy poison tested.

*Compounds previously tested.[29]

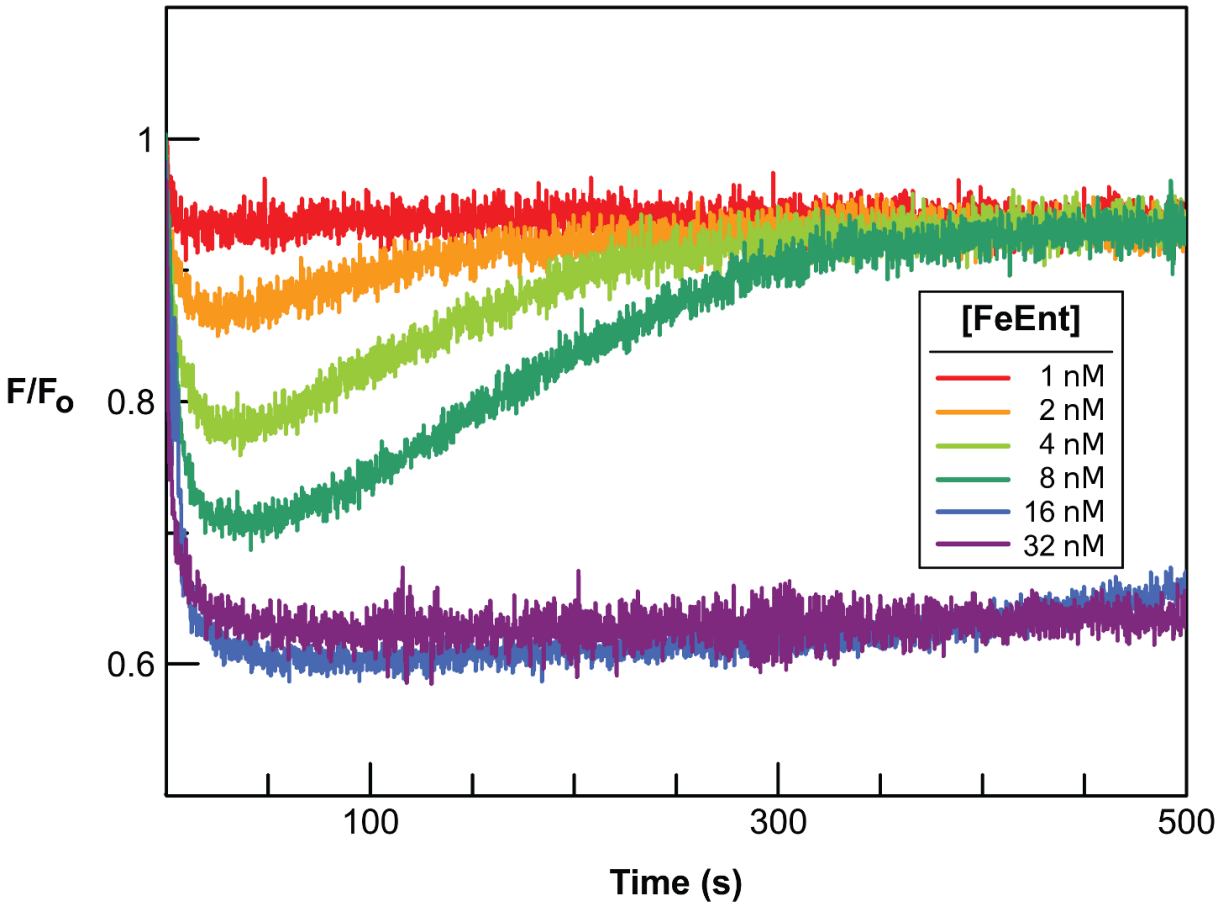

Figure 4.4 FeEnt concentration dependence on fluorescence properties

Fluorescence of OKN3/pFepAS271C cells was quenched with variable concentrations of FeEnt 1 nM (red), 2 nM (orange), 4 nM (yellow), 8 nM (green), 16 nM (blue), and 32 nM (purple). The extent of fluorescence quenching and rate of fluorescence recovery were concentration dependent.

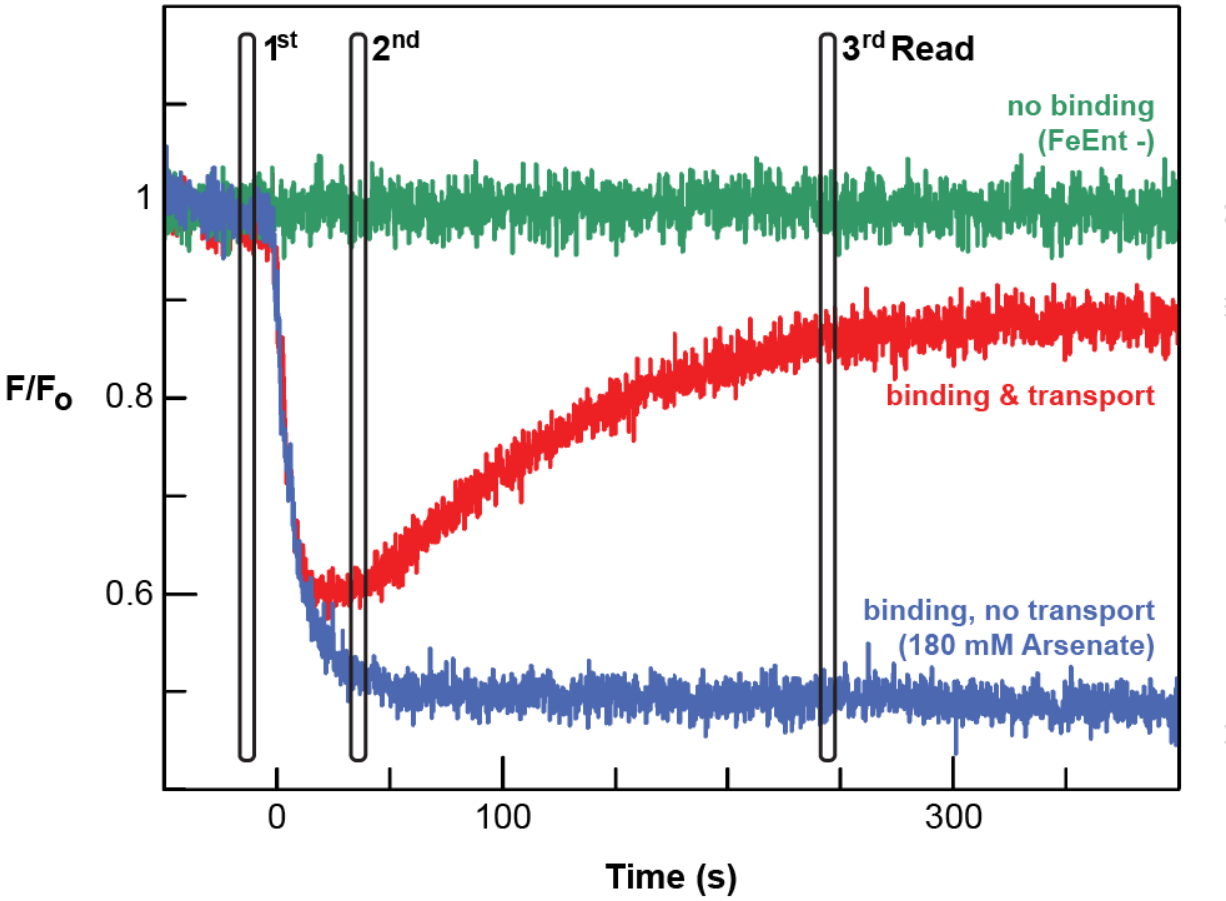

Figure 4.5 HTS assay design

Assay concept distinguishes between no FeEnt binding (green), binding with transport (red), and binding without transport (blue). Measurement times denoted by black rectangles.

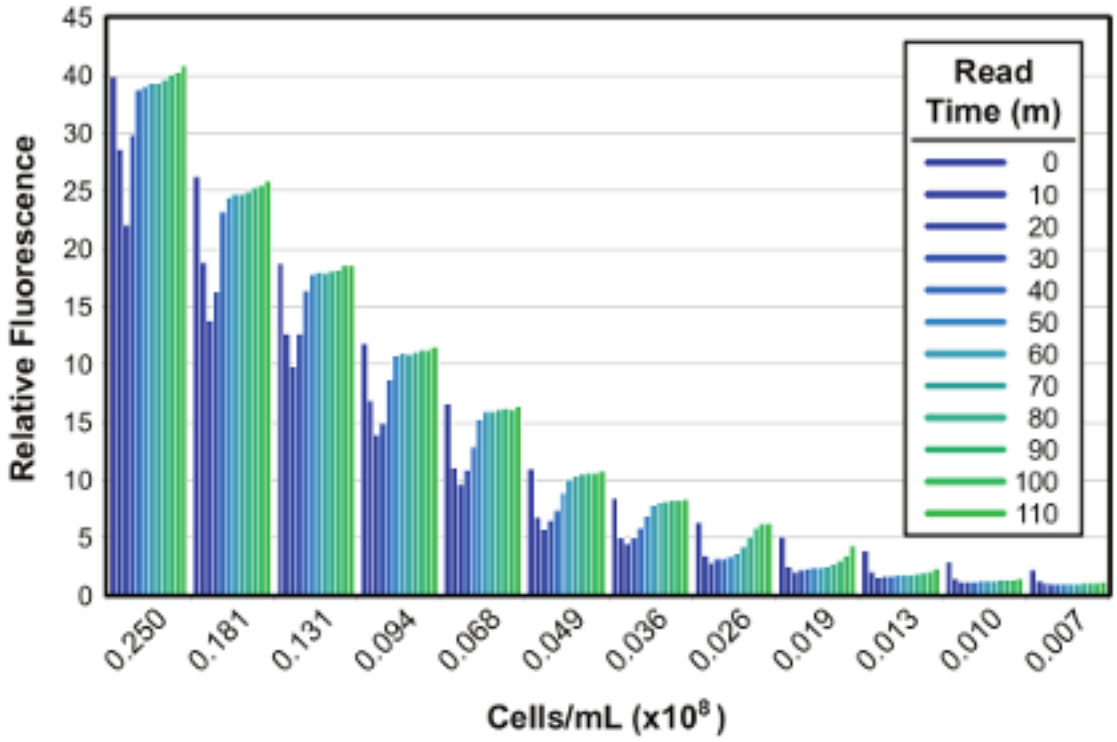

Figure 4.6 Cell density dependence of signal fluorescence properties

Fluorescence of OKN3/pFepAS271C cells quenched with 200 nM FeEnt. Fluorescence intensity was observed over 110 minutes (blue to green). Cell density of sample ranged from 0.250 to 0.007 cells/mL (x10^8).

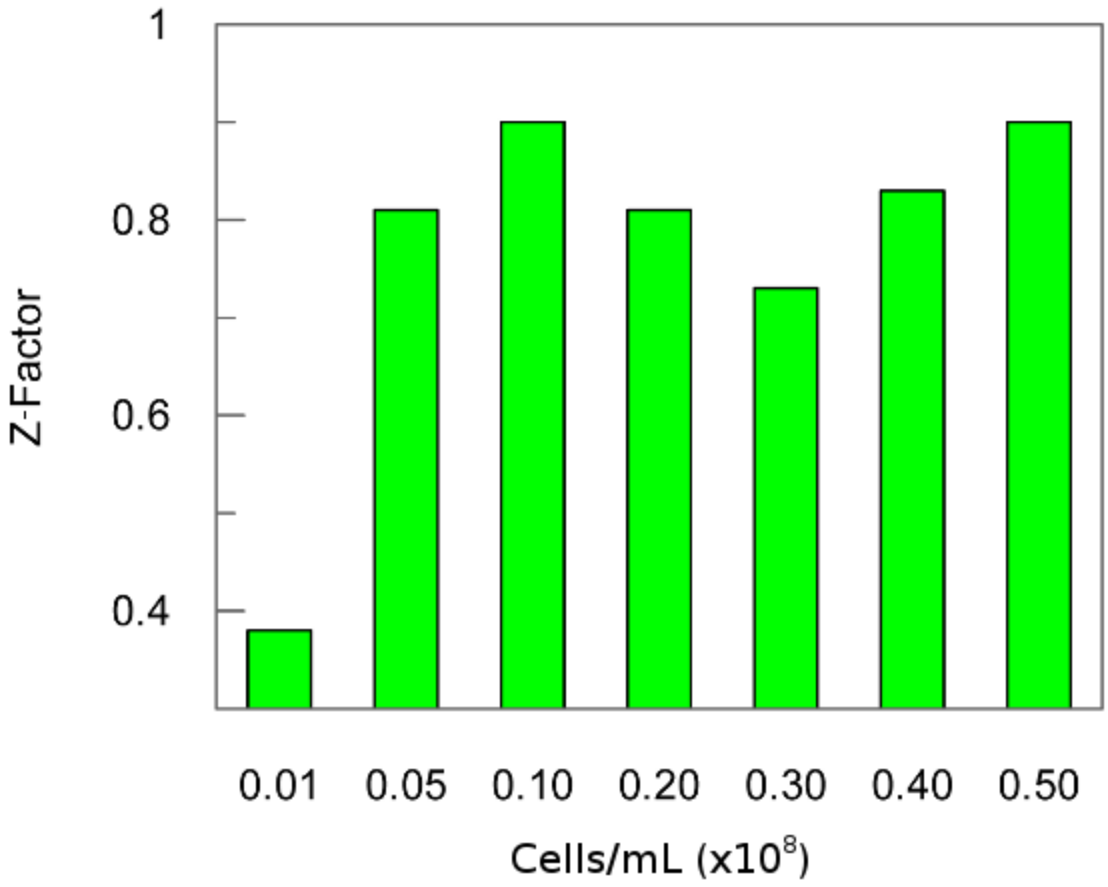

Figure 4.7 Z-factor dependence on cell density

We calculated the Z-factor for samples with variable cell densities (0.01, 0.05, 0.10, 0.20, 0.30, 0.40, and 0.50). The FeEnt concentrations used were dependent on cell density (Table 4.2).

Cell Density (Cells/mL (x10^8))	FeEnt Concentration (nM)
0.01	2
0.05	10
0.1	20
0.2	40
0.3	60
0.4	80
0.5	100

Table 4-2 Cell and FeEnt concentrations

Summary of Cell densities and FeEnt concentrations used in Z-factor determinations shown in Figure 4.7.

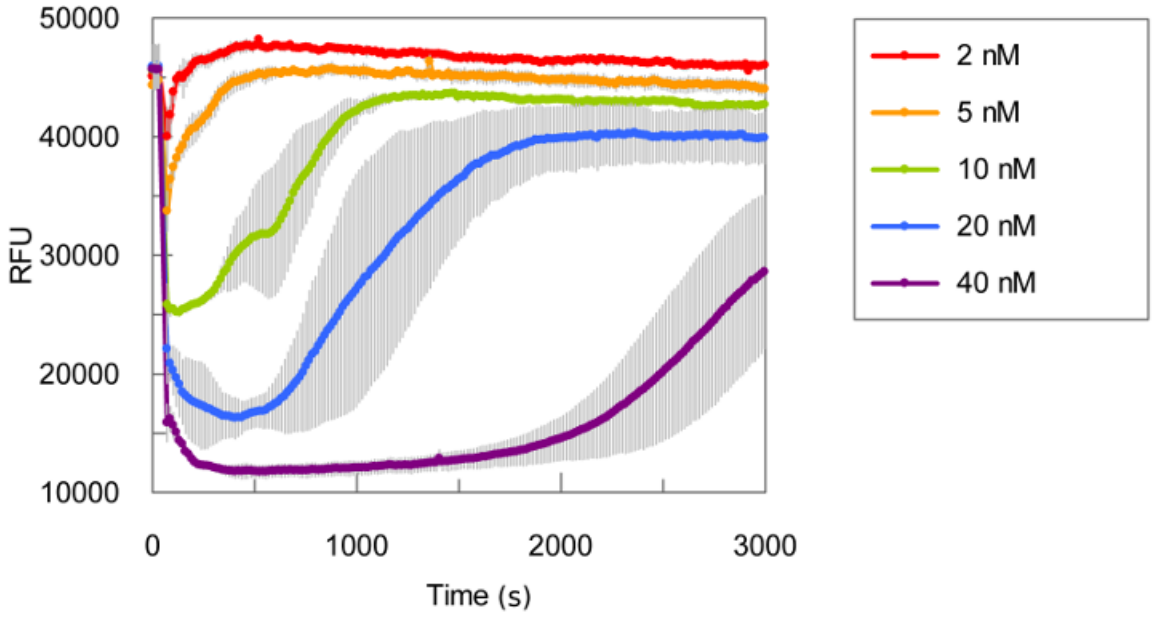

Figure 4.8 FeEnt concentration dependence on fluorescence properties

We quenched the fluorescence of OKN3/pFepAS271C cells with variable concentrations of FeEnt 2 nM (red), 5 nM (orange), 10 nM (green), 20 nM (blue), and 40 nM (purple) after the fifth measurement. The extent of fluorescence quenching and rate of fluorescence recovery were concentration dependent.

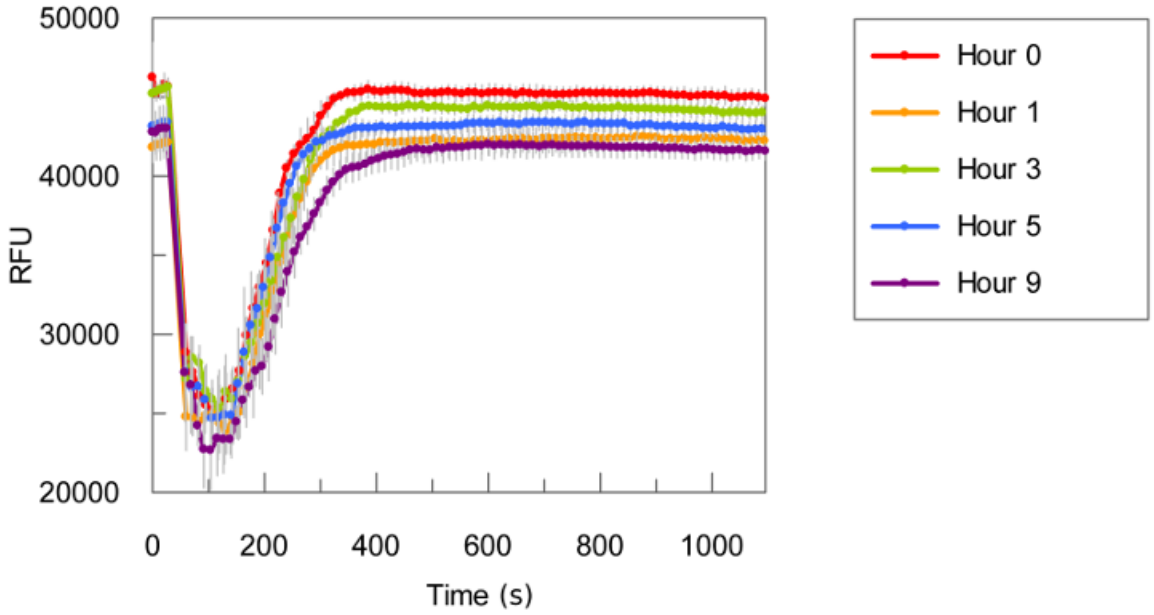

Figure 4.9 Cell stability

We analyzed aliquots samples of cells (0.1 Cells/mL (x10^8)) at the indicated time points (0 (red), 1 (orange), 3 (green), 5 (blue), and 9 (purple) hours) post fluorescent labeling. 20 nM FeEnt was added after the fifth measurement.

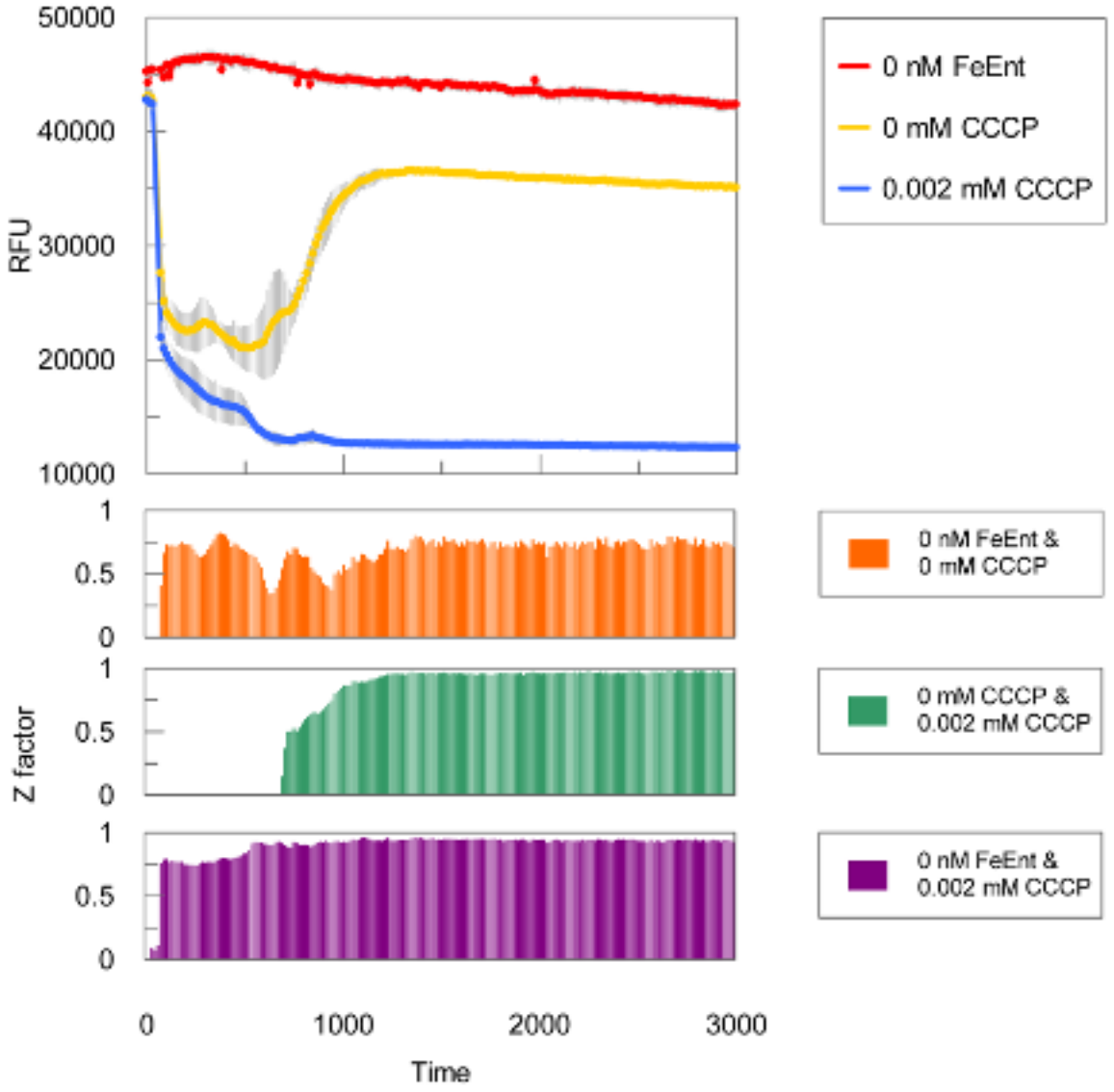

Figure 4.10 Control Stability

The fluorescence intensity of samples with (yellow and blue) or without (red) 20 nM FeEnt were analyzed over 50 minutes. FeEnt was injected after the fifth measurement. Samples were incubated with 0.002 mM CCCP (blue) or without (red and yellow). We performed Z-factor calculations at every time point between three controls (orange: red and yellow, green: yellow and blue, purple: red and blue)

Chapter 5 - Discussion

Using fluorescence spectroscopy of mutant FepA cell enabled us to determine the IC_{50} values for 3 energy poisons, and led to the development of a HTS assay for inhibitors of TonB-dependent iron acquisition. The IC_{50} concentration were found to be dependent on the type of energy poison. We used these data in the development of the HTS assay. Several different factors were evaluated during the optimization of the assay leading to a viable screening protocol.

The results for the energy poisons studied show a significant difference in the concentration required for 50% and 100% inhibition. Among the poisons tested CCCP had the lowest concentration for 50% inhibition at 0.05 mM and arsenate required 90 mM. This is likely due to the fact that the poisons affect different mechanisms within the cell. Arsenate is a phosphate analog that prevents ATP formation during one step of glycolysis. Sodium azide is an electron transport inhibitor that irreversibly binds to cytochrome proteins. DNP is a proton ionophore that prevents the formation of a proton gradient. CCCP also works by uncoupling ATP formation from the proton gradient. Cyanide is similar to sodium azide as it inhibits cytochrome c oxidase of the electron transport chain.

The energy poison data collected in this study is logically supported when compared to the mechanism of action of the various poisons. Proton motive force which energizes the translocation of FeEnt across the outer membrane via FepA is abolished by the two energy poisons which had the lowest inhibitory concentration. Poison that affect the electron transport chain by inhibiting cytochrome C such as

cyanide and sodium azide required higher concentration but far lower than the glycolytic poison arsenate. This is likely due to the fact that the cell is far more dependent on the electron transport chain in terms of the amount of ATP created.

In the development of the HTS assay several important factors needed to be investigated. In order to differentiate between the three possible outcome upon the introduction of FeEnt we determined three measurements were required: before addition of FeEnt, after addition of FeEnt, and after fluorescence recovery. However the energy poison data shows that at 2 nM the recovery of fluorescence after quenching may occur too rapidly before measurement on a HTS platform. By observing fluorescence quenching using 2 nM to 32 nM FeEnt we determined that increasing the concentration of FeEnt allows for an increased time prior to fluorescence recovery and an increase extent of quenching. This would allow for greater distinction between quenching and non-quenching events as the timing of measurements is critical.

The use of a HTS platform in the Tecan GENois pro allowed for greater flexibility and higher throughput in the development of the assay. To determine the correct concentration of cells used in the assay we determined the Z-factor over a range of cell concentrations. A concentration of 0.1 cells/mL ($x10^8$) was determined to be ideal. Most cell-based HTS assays use cell concentrations lower than this, but we determined that for this assay the Z-factor was significantly lower at more dilute concentrations. At 0.01 cells/mL ($x10^8$) the extent of quenching is less than the other samples. Higher concentrations had a similar Z-factor when compared to 0.1 cells/mL ($x10^8$), but may have increase turbidity. The mixing of sample wells may also become an issue at higher concentrations.

HTS campaigns can run for several hours so it was important to determine if the labeled cells would maintain a consistent fluorescence profile over this time frame. By evaluating aliquots over 9 hours we determined that the cells are stable when stored on ice. We observed little variation between any of the samples with regard to the extent of quenching or the speed of fluorescence recovery. If the HTS campaign runs for over 9 hours additional batches of cell would be prepared as needed. The variation between these cell batches could be accounted for by normalizing the data using the control samples.

The design of the controls is of particular importance in HTS field. To determine if an assay is viable the controls are used to calculate the Z-factor and to distinguish between positive and negative compounds. Hit selection is clearly vital when the number of tested compound can be in the thousands. Due to the multiple possible outcomes of this assay multiply controls were utilized. We observed the three controls over 50 minutes and calculated the Z-factor between each control. The differences in the fluorescence profile of the controls are apparent in the Z-factor calculations. By utilizing three measurement time points the three possible outcome can be observed. The timing of these measurement while critical allows for some flexibility. Other than the variable fluorescence recovery region of the 0 mM CCCP control the three controls exhibit stable fluorescence profiles over 50 minutes. The stability of these controls is important to the throughput of the assay as specific measurement times may be required based on the HTS instrumentation.

HTS is costly and therefore many factors must be considered before screening compounds. The viability of the assay to produce statistical significant results as

indicated by the Z-factor of approximately 0.7 is above the minimum guideline of 0.5 Z-factor. Our results indicate that statistical significant data can be obtained by this assay. Also with better instrumentation the Z-factor could increase during screening. We prepared all samples in this study using micropipettes, except for FeEnt injections on Tecan which were performed by the automatic injectors. HTS instrumentation with acoustic liquid dispensers would provide an increased level of precision over the Tecan Genios Pro. This increased precision would likely decrease the well-to-well variability in the assay and thus lead to a higher Z-factor.

Compared to other HTS assays the largest limitation of this assay is the lower throughput. Most assays will be inherently higher-throughput than this assay as they measure each well only one time, and measuring each well multiple times increases the amount of time for each plate to be read. The lowered throughput of the assay can be minimized by optimizing the timing of the measurements. For example, after pre-reading all plates for the pre FeEnt measurements each plate will have FeEnt injected and then read. After injection and reading of all plates the plates could be restacked and read for the final time. By processing the right number of plates per batch dependent on the instrumentation the length of time between the second and third measurements will allow for possibly fluorescence recovery and maximize throughput. Even with the most well designed assays can fail to yield positive leads; highlighted by the HTS for the drug Torcetrapib. 350,000 compounds were screened with only one hit.[25]

Another important consideration before a HTS campaign is the relevance of the data. Targeting bacterial iron acquisition is novel pathway for drug design due to the

importance of iron to bacterial pathogenicity. Another gram-negative bacteria, Yersinia enterocolitica, when injected with an iron-supplying compound increased in virulence approximately 10 million-fold.[33] The need for new antibiotic that target gram negative bacteria is likely to increase in the future due to antibiotic resistance, and any possible antibiotics that might result from this screening would be less likely to exhibit resistance as they affect a new bacterial target.[30] As FepA is characteristic of a TonB-dependent outer membrane transporter this novel assay may be generally used to identify inhibitors of TonB-dependent transport in other members of the Enterobacteriacae.[30] Not all HTS campaigns are successful and the absence of any known inhibitor of FepA is a concern. However, the multiple known ligands of FepA: FeEnt (700 Da), Colicin B (55 kDa), and Colicin D (75 kDa) suggest that FepA can bind structurally dissimilar compounds.[34] The mechanism by which these ligands are translocated by FepA is not entirely known and discovering new ligands may help to elucidate the transport properties of FepA.

Future Work

The future work related to this study will be running the assay at a HTS facility, and there are many factors which will need to be evaluated before choosing such a facility. Among these HTS instrumentation and compound library are of particular importance. The instrumentation must allow for the required plate handling and multiple measurements of each plate within one hour. As in all HTS tests the compound library is vitally important, and in particular in this assay due to the lowered throughput. Fewer compounds will be able to be tested so it must be ensured that the set of compounds

adequately samples the chemical space. Multiplexing may also be used the increase the throughput of the assay and not negatively affect results.

After running the assay the results will dictate what steps will need to be taken next. If proposed inhibitors of FeEnt binding or FeEnt transport are found after the HTS screening secondary assays will be performed to confirm the results. Iron transport assays with Fe^{59} can be used to verify interactions with possible inhibitors. Depending on the number of possible inhibitors found the Fe^{59} assay may also have to be adapted to a HTS format, if all compound are to be tested. Further testing may also include structural activity relationship (SAR) analysis, dose response, and cluster analysis.

References

(1) Silhavy, T. J.; Kahne, D.; Walker, S. The Bacterial Cell Envelope. *Cold Spring Harb. Perspect. Biol.* **2010**, *2*, a000414.

(2) Vollmer, W.; Blanot, D.; de Pedro, M. A. Peptidoglycan Structure and Architecture. *FEMS Microbiol. Rev.* **2008**, *32*, 149–167.

(3) Davies, J.; Davies, D. Origins and Evolution of Antibiotic Resistance. *Microbiol. Mol. Biol. Rev.* **2010**, *74*, 417–433.

(4) Messenger, A.; Barclay, R. Bacteria, Iron and Pathogenicity. *Biochem. Educ.* **1983**, *11*, 54–63.

(5) Raymond, K. N.; Dertz, E. A.; Kim, S. S. Enterobactin: An Archetype for Microbial Iron Transport. *Proc. Natl. Acad. Sci. U. S. A.* **2003**, *100*, 3584–3588.

(6) Theil, E. Ferritin: Structure, Gene Regulation, and Cellular Function in Animals, Plants, and Microorganisms. *Annu. Rev. Biochem.* **1987**, 289–315.

(7) Carrano, C.; Raymond, K. Ferric Ion Sequestering Agents. 2. Kinetics and Mechanism of Iron Removal from Transferrin by Enterobactin and Synthetic Tricatechols. *J. Am. Chem. Soc.* **1979**, *101*, 5401–5404.

(8) Ratledge, C.; Dover, L. Iron Metabolism in Pathogenic Bacteria. *Annu. Rev. Microbiol.* **2000**, *54*, 881–941.

(9) Neilands, J. Iron Absorption and Transport in Microorganisms. *Annu. Rev. Nutr.* **1981**, 27–46.

(10) Pollack, J. R.; Neilands, J. B. Enterobactin, an Iron Transport Compound from. *Biochem. Biophys. Res. Commun.* **1970**, *38*, 989–992.

(11) Nikaido, H.; Vaara, M. Molecular Basis of Bacterial Outer Membrane Permeability. *Microbiol. Rev.* **1985**, *49*, 1–32.

(12) Buchanan, S. K.; Smith, B. S.; Venkatramani, L.; Xia, D.; Esser, L.; Palnitkar, M.; Chakraborty, R.; van der Helm, D.; Deisenhofer, J. Crystal Structure of the Outer Membrane Active Transporter FepA from Escherichia Coli. *Nat. Struct. Biol.* **1999**, *6*, 56–63.

(13) Newton, S. M.; Igo, J. D.; Scott, D. C.; Klebba, P. E. Effect of Loop Deletions on the Binding and Transport of Ferric Enterobactin by FepA. *Mol. Microbiol.* **1999**, *32*, 1153–1165.

(14) Scott, D.; Newton, S.; Klebba, P. Surface Loop Motion in FepA. *J. Bacteriol.* **2002**, *184*, 4906–4911.

(15) Payne, M. A.; Igo, J. D.; Cao, Z.; Foster, S. B.; Newton, S. M. C.; Klebba, P. E. Biphasic Binding Kinetics between FepA and Its Ligands. *J. Biol. Chem.* **1997**, *272*, 21950–21955.

(16) Ma, L.; Kaserer, W.; Annamalai, R.; Scott, D. Evidence of Ball-and-Chain Transport of Ferric Enterobactin through FepA. *J. Biol. Chem.* **2007**, *282*, 397–406.

(17) Cao, Z.; Warfel, P.; Newton, S. M. C.; Klebba, P. E. Spectroscopic Observations of Ferric Enterobactin Transport. *J. Biol. Chem.* **2003**, *278*, 1022–1028.

(18) Klebba, P. E. Three Paradoxes of Ferric Enterobactin Uptake. *Front. Biosci.* **2003**, *8*, s1422.

(19) Jordan, L. D.; Zhou, Y.; Smallwood, C. R.; Lill, Y.; Ritchie, K.; Yip, W. T.; Newton, S. M.; Klebba, P. E. Energy-Dependent Motion of TonB in the Gram-Negative Bacterial Inner Membrane. *Proc. Natl. Acad. Sci. U. S. A.* **2013**, *110*, 11553–11558.
(20) Pawelek, P. D.; Croteau, N.; Ng-Thow-Hing, C.; Khursigara, C. M.; Moiseeva, N.; Allaire, M.; Coulton, J. W. Structure of TonB in Complex with FhuA, E. Coli Outer Membrane Receptor. *Science* **2006**, *312*, 1399–1402.
(21) Shultis, D. D.; Purdy, M. D.; Banchs, C. N.; Wiener, M. C. Outer Membrane Active Transport: Structure of the BtuB:TonB Complex. *Science* **2006**, *312*, 1396–1399.
(22) Sprencel, C.; Cao, Z.; Qi, Z.; Scott, D. C.; Montague, M. A.; Ivanoff, N.; Xu, J.; Raymond, K. M.; Newton, S. M. C.; Klebba, P. E. Binding of Ferric Enterobactin by the Escherichia Coli Periplasmic Protein FepB. *J. Bacteriol.* **2000**, *182*, 5359–5364.
(23) Chenault, S.; Earhart, C. Identification of Hydrophobic Proteins FepD and FepG of the Escherichia Coli Ferrienterobactin Permease. *J. Gen. Microbiol.* **1992**, *138*, 2167–2171.
(24) Silver, S.; Walderhaug, M. Gene Regulation of Plasmid- and Chromosome-Determined Inorganic Ion Transport in Bacteria. *Microbiol. Rev.* **1992**, *56*, 195–228.
(25) Pereira, D. A; Williams, J. A. Origin and Evolution of High Throughput Screening. *Br. J. Pharmacol.* **2007**, *152*, 53–61.
(26) Michelini, E.; Cevenini, L.; Mezzanotte, L.; Coppa, A.; Roda, A. Cell-Based Assays: Fuelling Drug Discovery. *Anal. Bioanal. Chem.* **2010**, *398*, 227–238.
(27) Paul, S. M.; Mytelka, D. S.; Dunwiddie, C. T.; Persinger, C. C.; Munos, B. H.; Lindborg, S. R.; Schacht, A. L. How to Improve R&D Productivity: The Pharmaceutical Industry's Grand Challenge. *Nat. Rev. Drug Discov.* **2010**, *9*, 203–214.
(28) Zhang, Z.; Guan, N.; Li, T.; Mais, D. E.; Wang, M. Quality Control of Cell-Based High-Throughput Drug Screening. *Acta Pharm. Sin. B* **2012**, *2*, 429–438.
(29) Smallwood, C. R.; Jordan, L.; Trinh, V.; Schuerch, D. W.; Gala, A.; Hanson, M.; Hanson, M.; Shipelskiy, Y.; Majumdar, A.; Newton, S. M. C.; Klebba, P. E. Concerted Loop Motion Triggers Induced Fit of FepA to Ferric Enterobactin. *J. Gen. Physiol.* **2014**, *144*, 71–80.
(30) Levy, S. B.; Marshall, B. Antibacterial Resistance Worldwide: Causes, Challenges and Responses. *Nat. Med.* **2004**, *10*, S122–S129.
(31) Saier, M. H. Families of Proteins Forming Transmembrane Channels. *J. Membr. Biol.* **2000**, *175*, 165–180.
(32) Zhang, J. H. A Simple Statistical Parameter for Use in Evaluation and Validation of High Throughput Screening Assays. *J. Biomol. Screen.* **1999**, *4*, 67–73.
(33) Robins-Browne, R.; Prpic, J. Effects of Iron and Desferrioxamine on Infections with Yersinia Enterocolitica. *Infect. Immun.* **1985**, *47*, 774–779.
(34) Masi, D. Di; White, J. Transport of Vitamin B12 in Escherichia Coli: Common Receptor Sites for Vitamin B12 and the E Colicins on the Outer Membrane of the Cell Envelope. *J. Bacteriol.* **1973**, *115*, 506–513.

Appendix A - Supplementary Figures

	Concentration (mM)															
Arsenate	1	5	10	20	40	60	80	100	120	130	140	150	160	170	180	200
Azide	1	2	3	4	5	6	7	8	9	10	11	13	15	16	18	
DNP	0.5	0.75	1	1.5	3											

Table A.1 Energy poison summary

Summary of energy poison concentrations tested.